WINDS FROM RED GIANT STARS

Observations and Modelling of Molecular Line Emission

Fredrik Larsen Schöier

Stockholm Observatory
Department of Astronomy
Stockholm University 2000

Doctoral Dissertation 2000
Department of Astronomy
Stockholm University
SE-106 91 Stockholm

Abstract:

Red giant stars are key objects in many astronomical fields of research. However, they are complicated objects and many physical and chemical processes combine to determine their properties. This makes it difficult to interpret the observations made towards these important stars, and to use them in a quantitative way when probing stellar evolution or galactic structure. A key process for their final evolution is mass loss from the surface, and this also has implications for the nucleosynthesis and the chemical evolution of galaxies. The mass loss leads to the formation of extended circumstellar envelopes of gas and dust particles, and their emission may be used to determine the mass loss characteristics.

We have performed extensive modelling of molecular line emission from the circumstellar envelopes using a detailed radiative transfer analysis. In particular, we present results on carbon monoxide radio line emission from a large sample of optically bright carbon stars. Assuming spherically symmetric envelopes created by a continuous, smooth expanding, mass loss, we are able to reproduce the observational results for about 90% of the sample stars. The derived mass loss rates span almost four orders of magnitude from roughly 5×10^{-9} up to 2×10^{-5} solar masses per year. The physical conditions prevailing in the circumstellar envelopes vary considerably over such a large range of mass loss rates, posing a challenge to the model. A comparison between the stellar and circumstellar properties is also provided. The majority of the remaining stars have known detached circumstellar envelopes, suggesting episodic mass loss.

Carbon stars are probably important in returning processed gas to the interstellar medium. We estimate that carbon stars of the type considered here annually return on the order of 0.05 solar masses of gas to the Galaxy, but more extreme carbon stars may contribute an order of magnitude more. However, as for the total carbon budget of the Galaxy, carbon stars appear to be of only minor importance.

We present estimates of the $^{12}C/^{13}C$-ratio towards a number of carbon stars. This carbon isotope ratio is an important probe of stellar evolution and, if known accurately, should increase our understanding of the processes that lead to the formation of carbon stars.

With the Infrared Satellite Observatory a new window for observing late-type stars was opened up, and this allowed studies of gas much closer to the star than was previously possible using, mainly, ground-based radio telescopes. By combining infrared and radio observations of carbon monoxide rotational lines we have been able to probe the circumstellar envelope characteristics over a large radial range. This provides a form of archaeology, giving a time resolved mass loss history of the object under study. In a similar way we have analysed stellar light scattered in circumstellar rotational-vibrational lines of

carbon monoxide.

Finally, we have also performed interferometric observations of the circumstellar line emission from hydrogen cyanide and cyanide, molecules with more complex spectra. Using a detailed treatment of the more complicated radiative transfer in these cases we are able to strengthen the observational constraints put on models describing the circumstellar chemistry.

ISBN 91-7265-111-3
Akademitryck AB, Edsbruk, 2000

Till Anna

Preface

This thesis presents studies of late stellar evolution. In particular, observations and modelling of circumstellar molecular line emission from red giant stars. The thesis is divided into two parts: The first section gives the reader a general introduction to the field, as well as a brief description of the radiative transfer code that has been developed to interpret the wealth of observational data obtained. The second part consists of reprints and preprints of the included scientific papers, as well as an appendix presenting observational material not yet published.

The thesis is based on the following six publications:

I. **Models of circumstellar molecular radio line emission**
Mass loss rates for a sample of bright carbon stars
Schöier F.L., Olofsson H., 2000, *A&A*, submitted

II. **The carbon star IRAS 15194-5115: circumstellar CO radio and FIR rotational lines**
Ryde N., Schöier F.L., Olofsson H., 1999, *A&A* **345**, 841

III. **The ^{12}C/^{13}C-ratio in cool carbon stars**
Schöier F.L., Olofsson H., 2000, *A&A*, in press

IV. **Modelling Mira's wind**
Ryde N., Schöier F.L., 2000, *ApJ*, submitted

V. **The young detached CO shell around U Camelopardalis**
Lindqvist M., Olofsson H., Lucas R., Schöier F.L., Neri R., Bujarrabal V., Kahane C., 1999, *A&A* **351**, L1

VI. **Molecular envelopes around carbon stars**
Interferometric observations and models of HCN and CN emission
Lindqvist M., Schöier F.L., Lucas R., Olofsson H., 2000, *A&A*, submitted

Contents

Chapter 1

Introduction

1.1 AGB-stars

Red giant stars evolving along the asymptotic giant branch (AGB) are in their final stellar phase. This is the endpoint for the large majority of all stars in the universe that have left the main sequence. AGB stars are among the most luminous stars, contributing significantly to the integrated starlight of galaxies, and their high luminosity and age make them ideal for probing the structure and dynamics of galaxies. Beyond the direct astronomical interest is the fact that our Sun will be going through this stage in about eight billion years.

AGB-stars lose copious amounts of matter ($\sim 10^{-8}$–$10^{-4}\,M_\odot\,yr^{-1}$) in an intense stellar wind. In fact, it is the mass loss that determines the AGB lifetime and not the nuclear burning processes. While the overall picture regarding the evolution of these red giant stars is fairly well understood, some of the underlying physical processes are not. Much of the difficulties are connected with the intense mass loss. Hence, a determination of the mass loss characteristics, i.e., the dependence on time, mass, chemistry, metallicity, etc., is of utmost importance for our understanding of late stellar evolution. In addition, an understanding of the atmospheric and circumstellar chemistry is required to determine the elemental abundances in these winds, which contribute to the chemical evolution of the interstellar medium (Busso et al. 1999). Finally, since AGB stars are the progenitors of planetary nebulae (PNe), the CSEs are very likely important ingredients in the formation of PNe (Kwok 1993).

The primary observational consequence of the mass loss is the creation of a circumstellar envelope (CSE) of gas and dust around the star. The low temperature of the central star allows the formation of a wide variety of molecular species in its atmosphere and expanding CSE. The chemistry of the latter can be very rich and depends on the C/O-ratio, the thickness of the envelope, and the ambient ultraviolet field. The study of these CSEs is crucial to our understanding of the late stages of stellar evolution. It will also allow us to determine the properties of higher mass loss rate objects, for which the central star may be completely obscured.

Observations of molecular millimeter wave line emission have proven to be one of the best tools for studying the structure, kinematics, and chemistry of the CSEs (Olofsson 1996a). With the advent of space-born observatories it is now possible to trace the molecular gas closer to the central star, thereby probing the complex inner parts of the envelope. These kinds of observations will, in the prolongation, help us to understand the underlying physical mechanisms responsible for the mass loss. The numerical modelling of these interesting systems, where intricate interplays between physical and chemical processes take place, is a challenge, and will, with the help of new technology observations, continue to be so for some time.

1.2 Evolution of low- to intermediate-mass stars

AGB-stars are the decendants of main-sequence (MS) stars with masses in the range $\sim$1$-$10 $M_{\odot}$. In what follows a general description of the evolution of these stars will be given, with special remarks made to the predicted evolution of one of these stars, namely our own Sun (Figure 1.1; Sackmann et al. 1993).

Stars are born from gravitationally contracting interstellar clouds of gas and dust. Much of the details of the advent of a star is still uncertain and will not be discussed here. We will instead start to follow the star as it settles on the MS. By this time hydrogen burning in the stellar core has started and the luminosity of the star is solely determined by the nuclear burning reactions. At this stage the star can be described as consisting of two distinct parts; a hot and dense core, where hydrogen is converted to helium, surrounded by a mantle consisting mainly of hydrogen. The continued evolution of the star will be affected by the close relationship between these two parts. The MS is by far the longest and most stable phase during a star's life. The age of the Sun is about 4.5 Gyr and is marked by a circle in Figure 1.1. The Sun will spend about an additional 6.4 Gyr on the MS before its central hydrogen supply is exhausted. During the MS the Sun's luminosity will change from 0.7$-$2.2 $L_{\odot}$, i.e., about a factor of three over $\sim$11 Gyr (these stable conditions on the surface of the Sun has allowed for the development of life on Earth). As the MS phase ends, when central hydogen is exhausted, stellar evolution speeds up considerably and the star enters the violent path leading to its inevitable death.

With no nuclear reactions to support it the core will contract and heat up due to the release of gravitational potential energy. Eventhough nuclear fusion in the core is extinguished, hydrogen is actively burning in a surrounding shell. The core contraction will allow the hydrogen shell to burn faster. The extra amount of energy produced in this way is first used almost entirely to expand the star, but soon, as the contraction of the core speeds up, also the surface luminosity will increase drastically and the star starts to ascend the red giant branch (RGB), evolving towards lower temperatures and larger radii (making it a red giant). During the RGB evolution the convective mantle will reach down to areas having experienced hydrogen burning. This will mix processed material to the surface, altering the chemical composition in the stellar atmoshere, in an event called the first dredge-up.

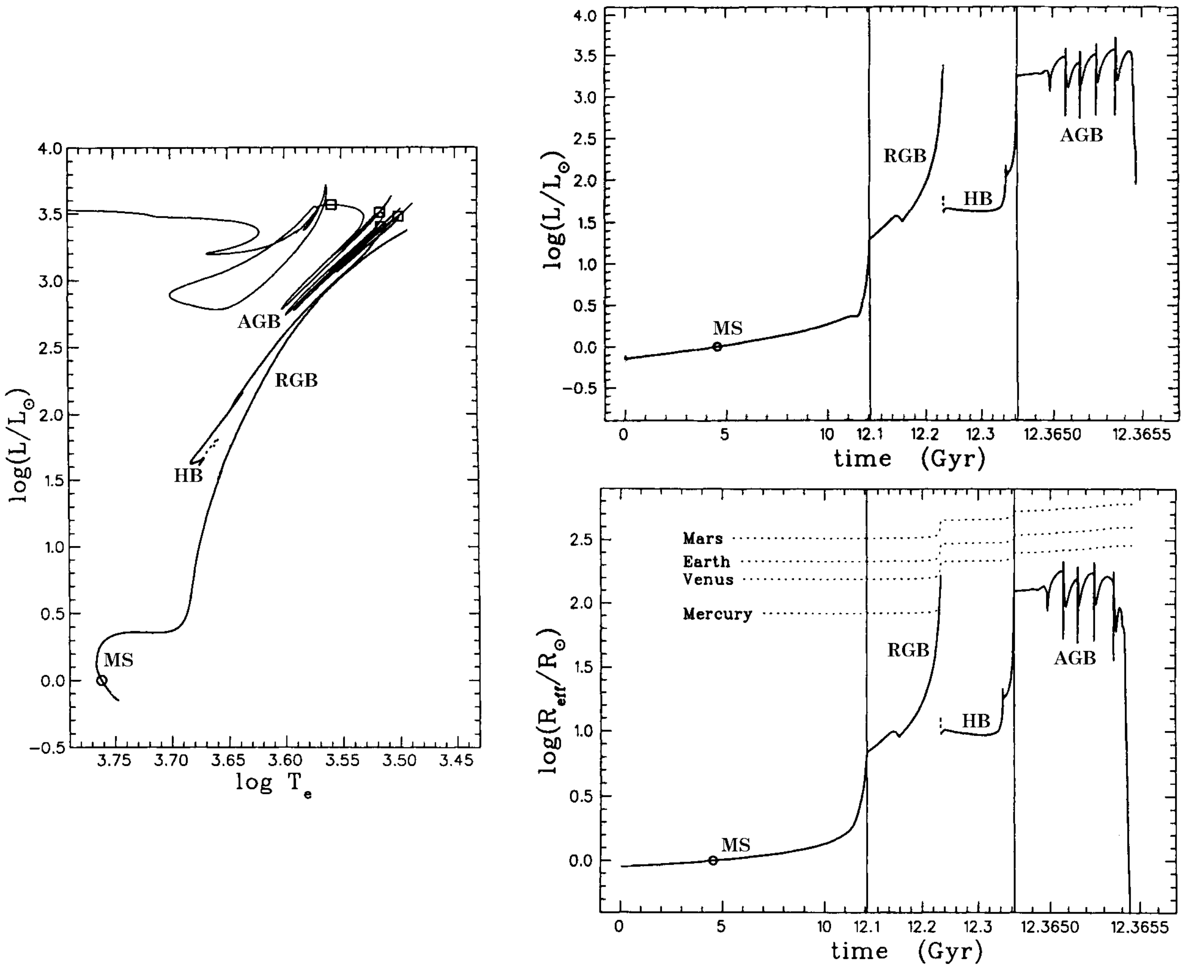

Figure 1.1: The predicted evolution for our Sun [adopted from Sackmann et al. (1993)]. Shown here is the evolution in the Hertzsprung-Russel diagram (left), of the luminosity (upper right), and of the effective stellar radius (lower right). The circle in these panels show the present Sun and the main evolutionary branches are indicated (see text for details). The rapid oscillations present during the AGB stage in all the panels are due to helium-shell flashes (thermal pulses). In the figure showing the predicted evolution of the Sun's radius, planetary orbits are shown for comparison (note the changes in the planetary orbits due to a decrease of the Sun's mass; a result of mass loss).

At the tip of the RGB the luminosity of the Sun will have grown to about $2350\,L_\odot$ in just 0.6 Gyr, and its radius has increased dramatically, now gracing the orbit of Venus in this particular model of the Sun (Figure 1.1). The central contraction have now produced a hot, dense, core, which will allow helium to ignite. For a low-mass star ($M \lesssim 2\,M_\odot$) the core has become electron-degenerate, with the help of energy losses via neutrinos. The huge amount of energy released at the onset of the thermonuclear reactions will be used to lift the degeneracy of the core further increasing the temperature and hence speed up the nuclear burning reactions, ultimately leading to a thermonuclear runaway (normally, as is the case for intermediate-mass stars, under non-degenerate conditions the energy released would go into expansion of the core instead of raising the temperature, thereby controlling the nuclear burning process and preventing a runaway). The runaway process produces, what is known as, a helium-core flash occurring at the tip of the RGB. The huge amount of energy released in this violent event completely removes the degeneracy in the core, and greatly expands the star. The expansion of the star cools the hydrogen burning shell leading to an actual decrease of the surface luminosity during this event. For stars more massive than $\sim 2\,M_\odot$ the core will be hot enough to prevent it from evolving into a degenerate state.

Eventually, the star will settle down on the horizontal branch (HB), quiescently burning helium in its core. For the Sun this second relatively calm period lasts only for about 0.1 Gyr, i.e., $\sim$1% of its MS life time. When the central helium supply is finally exhausted the core will start to contract, causing the stellar luminosity to increase and the star to expand, i.e., it becomes a red giant star for the second time. This is the early evolution on the AGB. Helium will continue to burn in a shell, surrounding the core, but located inside the hydrogen burning shell. Thus the star will effectively have divided itself into a double-shell burning star (Figure 1.2). At the early AGB helium burning dominates, but eventually hydrogen will burn more effective gradually increasing the luminosity. The star now evolves along the AGB. The central parts, by now a carbon-oxygen core, continues to contract until they finally become electron-degenerate. The scenario of a helium burning shell inside a hydrogen burning shell is unstable (Iben & Renzini 1983). In a recurrent event, known as a helium-shell flash, the helium shell will experience thermonuclear runaways with a local energy generation of $\sim 10^6\,L_\odot$. This energy first goes into a rapid expansion of the star, which quenches the hydrogen burning shell, leading to an actual drop in surface luminosity. After a few hundred years, however, the surface luminosity will increase drastically as the energy produced in the thermonuclear runaway reaches the surface of the star. As the helium-shell flash dies out the surface luminosity gradually declines over a time scale of $\sim 10^4$ yr. Finally, the hydrogen burning shell will reignite causing the luminosity to gradually increase again. The interpulse time scale is estimated to be approximately 10^5 yr for a star of about a solar mass. The star is now said to be on the thermally pulsing AGB (TP-AGB). In the model of the Sun presented in Figure 1.1 four helium-shell flashes will occur during the TP-AGB, which lasts $\sim 4\times 10^5$ yr. During the TP-AGB the convective mantle may reach down into the intershell region, and in a third dredge-up bring freshly nucleosynthesized material to the surface, which eventually may change the C/O-ratio leading to the formation of a carbon star for which C/O>1.

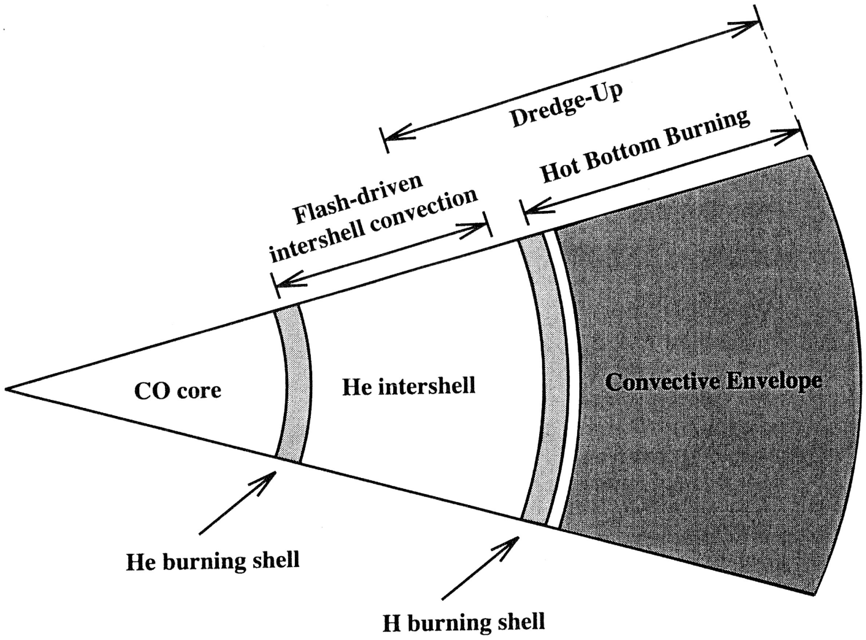

Figure 1.2: Schematic picture of the interior parts of an AGB-star [adopted from Lattanzio & Forestini (1999)].

For stars more massive than $\sim 4\,M_\odot$ the convective part of the mantle will reach down to hydrogen exhausted layers bringing processed material to the surface of the star. This mixing process is called the second dredge-up. The bottom of the convective mantle can reach and even penetrate the hydrogen burning shell leading to a nuclear burning process called hot bottom burning (HBB) (e.g., Boothroyd et al. 1993; Lattanzio & Forestini 1999). Models of HBB predict that this process effectively destroys ^{12}C, while producing ^{14}N and ^{13}C. One observational signature of a star having experienced HBB would be a relatively low ^{12}C/^{13}C-ratio of $\sim$3$-$5, i.e., close to the equilibrium value for the CNO-cycle (see **Paper II** for a candidate star).

During the AGB the mantle starts to lose material at an increasing rate, producing an extended envelope of gas and dust around the star. The mass loss will affect both the future evolution of the core and the nuclear burning regions in the envelope, and from now on mass loss dictates the evolution and not the nuclear burning processes. In the model of the Sun peak mass loss rates of $\sim 2.5\times10^{-7}\,M_\odot\,\mathrm{yr}^{-1}$ are reached but this is highly model dependent. One expects most of the material to be lost a the peak of the AGB, a superwind phase, leaving in the centre , an inert and bare C/O-core, a cooling white dwarf (WD). The future WD remnant of the Sun is expected to have a mass of $\sim 0.5\,M_\odot$, i.e., roughly half of the initial MS mass will have been lost during the rapid stellar evolution as a red giant. The rapid increase in stellar surface temperature when the core is uncovered, produces an energetic radiation field, which ignites the escaping circumstellar envelope and a PN is formed.

1.3 Mass loss

A typical AGB-star has a radius of $\sim 3\times10^{13}$ cm (=2 AU), a luminosity of $\sim 6000\,L_\odot$, an effective temperature of ~ 2500 K, and its luminosity is variable with large amplitudes and long periods $\sim 50-500$ days. The pulsational behaviour, forcing the star out of hydrostatic equilibrium, is thought to play an important role in the intense mass loss experienced by these stars (see Figure 1.3). The pulsation will induce shock waves which propagate through the stellar atmosphere, and in doing so dissipate their energy gradually. This will levitate the atmosphere, thereby cooling it. In the cooling outflow, where a complex chemistry is now taking place, solid dust particles will start to develop. Once dust is able to form, the characteristics of the envelope will change. The macroscopic dust particles will effectively absorb stellar photons at short wavelengths and re-emit them at longer wavelenghts, producing an observable infrared excess in the spectrum of the star. The momentum transferred from the absorbed photons to the dust will effectively accelerate the dust particles outward. The gas is momentum coupled, through collisions, to the dust, and it will be effectively dragged along by the dust, leading to the observed gas mass loss rates of $\sim 5\times10^{-8}-2\times10^{-5}\,M_\odot\,\mathrm{yr}^{-1}$ at wind velocities of $\sim 10-20\,\mathrm{km\,s}^{-1}$ (**Paper I**). The momentum coupling will also effectively heat the surrounding gas.

The mass loss produced in this way seems to be close to isotropic, although not entirely homogeneous, as there are indications of a clumpy medium (e.g., Olofsson et al. 1996b, 2000; Neri et al. 1998; **Paper V**). The isotropy of these outflows is also supported by the success in modelling the large number of AGB stars, presented in this thesis, using a spherically symmetric CSE. The overall spherical symmetry prevailing for AGB-stars is in clear contrast to post-AGB objects, where axi-symmetric outflows are common.

The central stars of some AGB stars appear to have been subject to drastic modulations of their mass loss rates over relatively short periods of time (a few thousand years), which produced detached CSEs (dCSEs; Olofsson et al. 1996b; **Paper V**). Presently, these stars are losing matter at a significantly lower rate, forming what is referred to as an attached circumstellar envelope. It is estimated that the dCSE CO-line emission is observable for $\sim 10^4$ years (Bergman et al. 1993). If this mass ejection is a repeatable phenomenon, and all AGB stars go through this phase, the estimated time scale between mass ejections is about 10^5 years. Therefore, the mass ejections may possibly be linked with the helium-shell flashes predicted to occur regularly in AGB stars with time intervals of the order of 10^5 years for solar mass stars (e.g., Blöcker 1995).

1.4 The carbon star phenomenon

The carbon star phenomenon, i.e., the presence of stars for which the abundance of carbon exceeds that of oxygen in the atmospheres, occurs during the final AGB evolution. Current theoretical models of stellar evolution on the AGB predict that stars with "normal" chemical composition transform into carbon stars, i.e., from spectral type M, via the intermediate spectral types MS, S and SC, through the dredge-up of freshly synthesized

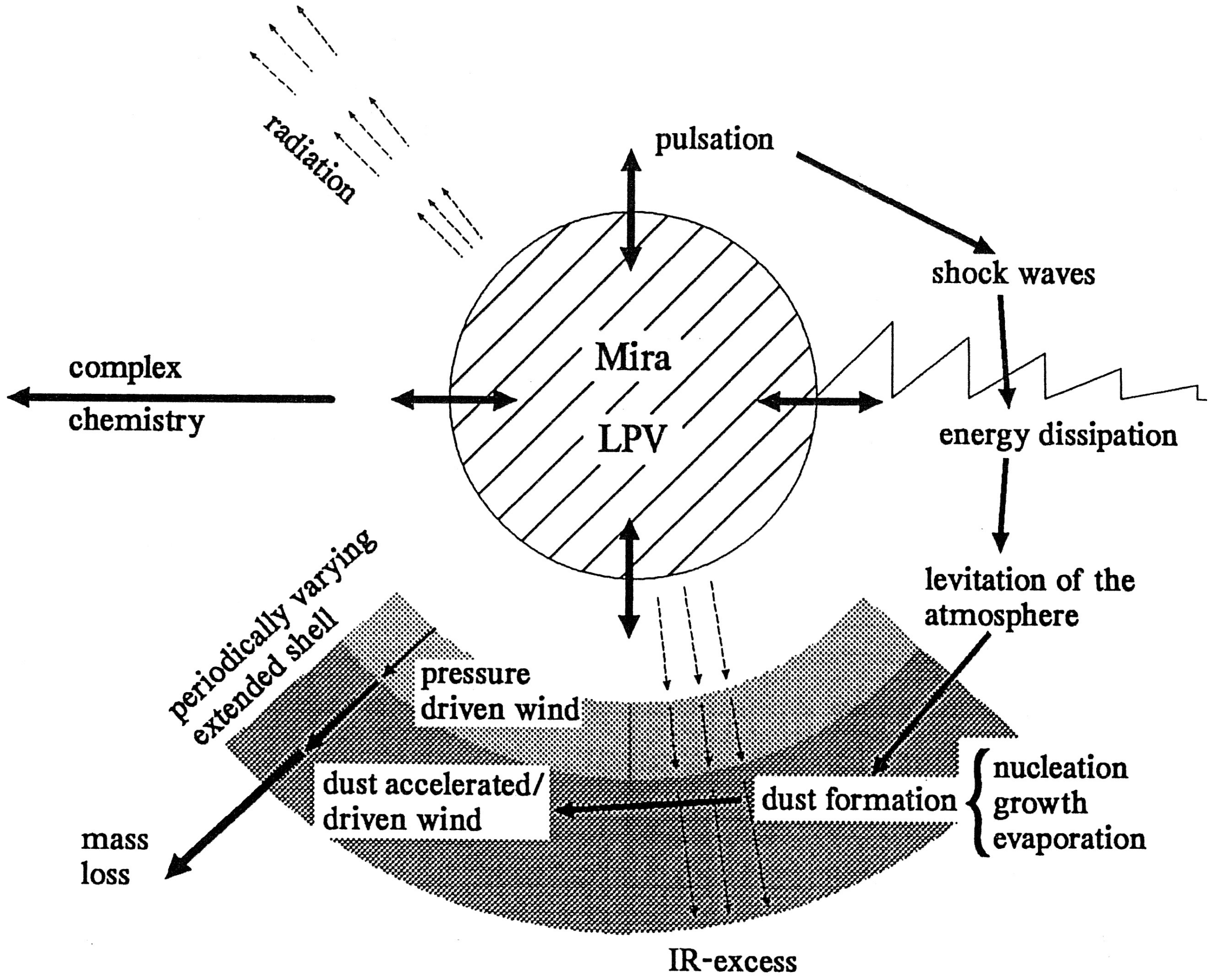

Figure 1.3: Schematic picture of the mass loss mechanism [adopted from Sedlmayr (1990)]. It is thought to act through a two-stage process, where shock waves levitate the atmosphere so that dust grains can form, and radiation pressure on the dust grains accelerates the wind. The momentum picked up by the dust particles is transferred to the gas, leading to expansion and heating of the gas.

carbon in He-shell flashes (Busso et al. 1999). This scenario is also confirmed by observations (e.g., Lambert et al. 1986), using the ^{12}C/^{13}C-ratio as a measure of stellar evolution and nucleosynthesis. Since mainly the ^{12}C-isotope is synthesized, there should be a coeval evolution in the ^{12}C/^{13}C-ratio from the value determined during the first red giant evolution. In addition, processes like hot bottom burning will affect this ratio, as well as set an upper mass limit for carbon stars. Thus, an accurate estimate of the ^{12}C/^{13}C-ratio should increase our understanding of the processes that lead to the formation of carbon stars (e.g., Forestini & Charbonnel 1997; Wallerstein & Knapp 1998). In **Paper III** we determine this ratio for a number of carbon stars using the circumstellar CO emission, which we believe to accurately measure the stellar $^{12}C/^{13}C$-ratio, and find ratios in the range 2.5 to 90. The $^{12}C/^{13}C$-ratio is also an important tracer of the past starformation rate and stellar mass function (Prantzos et al. 1996; Greaves & Holland 1997).

One of the main conclusions in **Paper I**, which is based on observations of a relatively complete sample within 1 kpc of the Sun (Olofsson et al. 1993), is that probably all carbon stars lose mass at a detectable rate, i.e, more than $\sim 1\times10^{-8}\,M_\odot\,yr^{-1}$. Although there is a large spread in mass loss rates for carbon stars, over four orders of magnitude, the distribution appears sharply peaked around $\sim 1.5\times10^{-7}\,M_\odot\,yr^{-1}$. Interestingly, this is about the same rate at which the core mass is expected to grow (Schönberner 1983), intimately linking the mass loss rate to the evolution of the star. The physical conditions prevailing in the CSEs vary considerably over the large observed range of mass loss rates. Among other things, it appears that the dust-to-gas mass ratio and/or the dust properties change with the mass loss rate. We find that the mass loss rate and the gas expansion velocity are relatively well correlated, and that both depend on the stellar luminosity. Moreover, the mass loss rates correlate well with the stellar pulsational period, indicating that variability is an important ingredient in the mass loss mechanism. Finally, we find that the mass loss rate also correlates weakly with the stellar effective temperature, in the sense that the cooler stars tend to have higher mass loss rates, but there seems to be no correlation with the stellar C/O-ratio.

Carbon stars are probably important in returning processed gas to the ISM. In **Paper I** we estimate that optically bright carbon stars, located on the AGB, annually return at least $\sim 0.05\,M_\odot$ of gas to the Galaxy. However, as for the total carbon budget of the Galaxy, they appear to be of only minor importance.

1.5 Observing circumstellar envelopes

Molecular line radiation from CSEs has been detected in various wavelength regimes, from the ultraviolet to radio, both as quasi-thermal and highly non-thermal, i.e., maser, radiation. An expanding CSE was first detected in the visual regime by Deutsch (1956), who interpreted circumstellar lines around the binary M-star α Her as a sign of mass loss. One of the advantages with optical observations is the usually good angular resolution, e.g., scattered light observations of NaI and KI provide information on the radial structure of the inner region of a CSE (Gustafsson et al. 1997). However, observations of molecular millimetre line emission and thermal infrared continuum radiation from dust particles have proven to be the best ways in which to study CSEs, thereby drastically increasing our knowledge of late stages of stellar evolution. While non-thermal maser emission from various molecules (SiO, H_2O, and OH) has proven to be a useful tool to probe the CSEs of oxygen-rich stars (Habing 1996), the study of carbon star envelopes has relied almost entirely on thermal radiation (Wallerstein & Knapp 1998). Both types of stars have also been extensively studied in circumstellar dust emission; here the IRAS survey, ISO observations, and other dedicated IR surveys have added considerably to our understanding of late stellar evolution.

The first detection of thermal molecular line emission was done in the CO(J=1$\rightarrow$0) transition from the CSE around the high mass loss rate Mira variable IRC+10216 (Solomon et al. 1971).Presently, ~60 different molecular species have been identified in CSEs around AGB-stars (Olofsson 1997). Recently, interferometer observations, e.g., using the Plateau de Bure interferometer, havw provided us with high spatial resolution information (~1$''$) for a growing number of CSEs also at millimeter wavelengths (e.g., Neri et al. 1998; **Papers V & VI**).

Far-infrared observations, using the Infrared Space Observatory (ISO), have further increased our knowledge of AGB-stars. E.g., with ISO it is possible to sample high-energy rotational transitions originating from the inner parts of CSEs (**Paper II**). Moreover, new technologies also make it possible to observe molecular line emission in the near-infrared from ground-based telescopes, such as CO rotational-vibrational lines (**Paper IV**). This kind of observations also provide detailed spatial information on the distribution of the molecular gas.

Since the radiation observed in various wavelength regimes samples gas at different temperatures, one is able to probe different radial regimes in the CSE. The combination of multi-wavelength observations and a radiative transfer model, for their interpretation, is therefore a very powerful tool in the study of CSEs (**Papers II & IV**; Section 3.3).

Chapter 2

Radiative transfer

Astronomy is mainly an observational science where electromagnetic radiation is the most important messenger of the physical conditions prevailing in the astronomical object under study. Thus, it is of utmost importance to understand the propagation of this radiation and how it interacts with matter. In this chapter the formalism used to interpret the observed radiation will be reviewed.

2.1 The radiative transfer equation

Photons are the carriers of electromagnetic radiation. The fundamental macroscopic quantity used to describe the propagation of this radiation is the specific intensity I_ν. As a beam of light passes through a medium it will be subject to local emission and extinction events.

The radiative transfer equation for radiation propagating a distance, ds, can be written as

$$\frac{\mathrm{d}I_\nu}{\mathrm{ds}} = j_\nu - \alpha_\nu \, I_\nu, \tag{2.1}$$

where j_ν and α_ν are the local emission and extinction coefficients, respectively. A useful quantity for later use is the mean intensity

$$J_\nu = \frac{1}{4\pi} \int I_\nu \, \mathrm{d}\Omega, \tag{2.2}$$

i.e., intensity averaged over all directions. For future use we will introduce an, for radiation theory, important and useful quantity known as the source function

$$S_\nu \equiv \frac{j_\nu}{\alpha_\nu}. \tag{2.3}$$

Writing the transport equation in its integral form and defining the optical depth, $\mathrm{d}\tau_\nu \equiv \alpha_\nu \, \mathrm{d}s$, measured along the beam one arrives at

$$I_\nu^{\mathrm{em}} = I_\nu^{\mathrm{bg}} \, e^{-\tau_\nu} + \int_0^{\tau_\nu} S_\nu(\tau_\nu') \, e^{-(\tau_\nu - \tau_\nu')} \, \mathrm{d}\tau_\nu', \tag{2.4}$$

where $I_\nu^{\rm em}$ is the radiation emerging from the medium and $I_\nu^{\rm bg}$ is the radiation entering the medium.

Spectral lines arise when the local emission and absorption properties change drastically over a very small frequency interval, due to the presence of molecules (or atoms). From now on we will focus on bound-bound transitions within a multi-level molecule consisting of N levels with spontaneous downward rates A_{ul}, Einstein coefficients for stimulated transitions B_{ul} and B_{lu}, and collisional rates C_{ul} and C_{lu}, between levels u and l.

The local emission, in transition $u \rightarrow l$ with laboratory frequency ν_{ul}, can then be expressed as

$$j_\nu = \frac{h\nu_{ul}}{4\pi}\, n_u\, A_{ul}\, \phi_\nu, \tag{2.5}$$

where n_u is the number density of molecules in level u and ϕ_ν is the frequency dependent line emission profile. The absorption coefficient reads

$$\alpha_\nu = \frac{h\nu_{ul}}{4\pi}\left(n_l\, B_{lu}\, \varphi_\nu - n_u\, B_{ul}\, \chi_\nu\right), \tag{2.6}$$

where ϕ_ν and χ_ν are the line profile for absorption and stimulated emission (counted as negative extinction), respectively.

In what follows we will assume complete angular and frequency redistribution (CRD) of the emitted photons. The assumption of CRD implies that $\phi_\nu = \varphi_\nu = \chi_\nu$, and is valid in the case where collisional excitation dominates. However, it appears also to be a good approximation in some cases where it is strictly not applicable (**Paper IV**). This will allow the source function to be written as

$$S_\nu = \frac{n_u A_{ul}}{n_l B_{lu} - n_u B_{ul}} = \frac{2h\nu_{ul}^3}{c^2}\left(\frac{g_u n_l}{g_l n_u} - 1\right)^{-1}, \tag{2.7}$$

where we have used the Einstein relations, and introduced the statistical weights g of levels u and l.

Thus, if one knows the level populations (n_i) the radiative transfer equation can be solved exactly. E.g., in local thermodynamic equilibrium (LTE) a knowledge of the temperature structure allows the determination of n_i. This is, for most astrophysical systems (including CSEs), generally not the case. In non-LTE problems statistical equilibrium (SE) is usually assumed

$$\frac{{\rm d}n_u}{{\rm d}t} = \sum_{l \neq u}^{N} n_l P_{lu} - n_u \sum_{l \neq u}^{N} P_{ul} = 0, \tag{2.8}$$

where

$$P_{ul} = A_{ul} + B_{ul}\overline{J}_{\nu_{ul}} + C_{ul}. \tag{2.9}$$

In Equation 2.9

$$B_{ul}\overline{J}_{\nu_{ul}} = B_{ul}\int_0^\infty J_\nu\, \psi(\nu)\, {\rm d}\nu \tag{2.10}$$

is the number of induced radiative de-excitations from state u to state l per second per particle in state u.

In circumstellar envelopes the dominant broadening mechanisms are turbulent and thermal broadening. This will produce a Gaussian line profile (e.g., Cannon 1985)

$$\phi_\nu = \frac{c}{\sigma\sqrt{\pi}} \exp\left[-\left(\nu - \nu_{ul} - \vec{v}\cdot\vec{n}\,\frac{\nu_{ul}}{c}\right)^2/\sigma^2\right], \tag{2.11}$$

where σ is the line width, $\vec{v}$ is the velocity vector of the moving gas at the position of the scattering, and $\vec{n}$ is a unit vector in the direction of the propagating beam of radiation.

2.2 The Monte Carlo method

In order to model the circumstellar emission and to derive the basic characteristics of the CSEs we have developed a non-LTE radiative transfer code based on the Monte Carlo method [Bernes (1979); further improved by Bergman (1985)]. The Monte Carlo method is well suited for the study of CSEs, since it is very flexible and close to the physics and yet simple in principle. For instance, one may include very complex geometries and velocity fields without being forced away from the physics of the problem.

The aim of the radiative transfer is to obtain the steady-state level populations, of the molecule under study, using the SE-equations. In the Monte Carlo method information on the radiation field is obtained by simulating the line photons using a number of model photons, each representing a large number of real photons from all transitions considered. These model photons, emitted locally in the gas as well as injected from the boundaries of the CSE, are followed through the CSE and the number of absorptions are calculated and stored. Photons are spontaneously emitted in the gas with complete angular and frequency redistribution (CRD), i.e., the local emission is assumed to be isotropic and the scatterings are assumed to be incoherent. The weight of a model photon is continuously modified, to take the absorptions and stimulated emissions into account, as it travels through the CSE. When all model photons are absorbed in, or have escaped, the CSE the SE-equations (Equation 2.8) are solved and the whole process is then repeated until some criterion for convergence is fulfilled. Once the molecular excitation, i.e., the level populations, is obtained the radiative transfer equation (Equation 2.4) can be solved exactly.

In what follows we will only, for simplicity, treat a two-level system but the generalization to a multi-level system is straightforward. The CSE is divided into a number of concentric spherical shells with their own set of physical parameters. At the point of its creation the model photon is assigned a weight, W, in proportion to the total number of real photons emitted. The optical depth experienced by a model photon as it travels a geometrical distance from x=0 to x=s_1 is (c.f., Equation 2.6)

$$\tau_1 = \frac{h\nu_{ul}}{4\pi}\phi_\nu\left(n_{l,m}B_{lu} - n_{u,m}B_{ul}\right)s_1 \tag{2.12}$$

The total number of induced de-excitations (stimulated emissions), $u \rightarrow l$ within a sub-shell m, that the model photon gives rise to is

$$N_{ul,m} = \frac{h\nu_{ul}}{4\pi}\phi_\nu n_{u,m} B_{ul} \int_0^{s_1} W(x)dx. \tag{2.13}$$

The weight of model photon at $x{=}s_1$ will be modified according to

$$W(s_1) = W_0 \exp(-\tau_1), \tag{2.14}$$

where W_0 is the weight at $x{=}0$. The number of stimulated emissions per molecule in the upper state, u, in shell m is

$$S_{ul,m} = \frac{N_{ul,m}}{n_{u,m}V_m} = \frac{h\nu_{ul}}{4\pi}\phi_\nu B_{ul}\frac{s_1 W_0}{V_m \tau_1}\left(1 - e^{-\tau_1}\right) \tag{2.15}$$

When all model photons have been emitted and followed throughout the CSE, $\sum S_{ul,m}$ will measure the total number of stimulated emissions per atom in the upper state u per second, i.e., we have gained information on Equation 2.10. We are now able to finally write the SE-equation (Equation 2.8), in Monte Carlo formalism, as

$$n_{l,m}\left(\frac{g_u}{g_l}\sum S_{ul,m} + C_{lu}\right) = n_{u,m}\left(A_{ul} + \sum S_{ul,m} + C_{ul}\right). \tag{2.16}$$

The desired level populations are obtained by solving the SE equation within each shell, m, using the additional constraint that $n_u{+}n_l$ is constant.

The main drawback of the Monte Carlo method is its slow convergence ($\sim\sqrt{N_{\mathrm{iter}}}$). This is, however, usually outweighed by its great adaptability. One of our motivations for choosing the Monte Carlo method was to be able to treat varying mass loss rates, departures from spherical symmetry, and the possibility of a highly clumped medium. These complicating issues will be investigated in a future version of our Monte Carlo code.

2.2.1 Line overlaps

When line overlaps occur the following modifications to to the original Monte Carlo concept must be made (González-Alfonso & Cernicharo 1993). The total opacity at frequency ν now becomes

$$\tau_1^{\mathrm{tot}} = s_1 \frac{h}{4\pi}\sum \nu_{u'l'}\phi_\nu(\nu_{u'l'})\left[n_{l',m}B_{u'l'} - n_{u',m}B_{u'l'}\right], \tag{2.17}$$

where the sum is taken over all transitions $\nu_{u'l'}$ which overlap at frequency ν.

Model photons emitted in transition ν_{ul} at frequency ν will induce radiative de-excitations as they travel the distance s_1 in the ν_{ul} transition

$$S_{ul} = s_1\frac{h\nu_{ul}}{4\pi}\phi_\nu(\nu_{ul})\frac{B_{ul}W_0}{V_m\tau_1^{\mathrm{tot}}}\left[1 - \exp\left(-\tau_1^{\mathrm{tot}}\right)\right], \tag{2.18}$$

as well as in all other transitions $\nu_{u'l'}$ which overlap frequency ν

$$S_{u'l'} = s_1 \frac{h\nu_{u'l'}}{4\pi} \phi_\nu(\nu_{u'l'}) \frac{B_{u'l'} W_0}{V_m \tau_1^{\rm tot}} \left[1 - \exp\left(-\tau_1^{\rm tot}\right)\right] . \quad (2.19)$$

These modifications were implemented in our radiative transfer code in order to model molecules where hyperfine structure leads to considerable (non-local) line overlaps between individual hyperfine components. With this addition to the code we are able in **Paper VI** to successfully model HCN and CN line emission (both molecules have a hyperfine structure) towards four carbon stars where detailed interferometer maps were obtained.

2.2.2 Testing the code

Due to the complexity involved when solving multi-level, non-LTE molecular excitation problems, any difficulties a particular radiative transfer code might run into can be hard to detect. A common problem for many radiative transfer algorithms is regarding convergence.

At a workshop, focusing on various radiative transfer algorithms for the interpretation of molecular line data, held in Leiden (The Netherlands) in 1999, a number of test problems[1] were defined in order to provide a possibility for detailed comparisons between various codes.

Presented in Figure 2.1 are the results for two of these test problems using our radiative transfer code. Problem 1 is a low abundance HCO^+ problem in a collapsing cloud model following the description given by Shu (1977). The parameters describing problem 2 are the same as those in problem 1 except for a higher abundance of HCO^+, significantly increasing the optical depths.

The radiative transfer code used in this thesis gives results, for these test problems, that are in excellent agreement with other existing models, such as, other Monte Carlo methods, (accelerated) lambda iterations, and MULTI.

[1] http://www.strw.leidenuniv.nl/~radtrans/

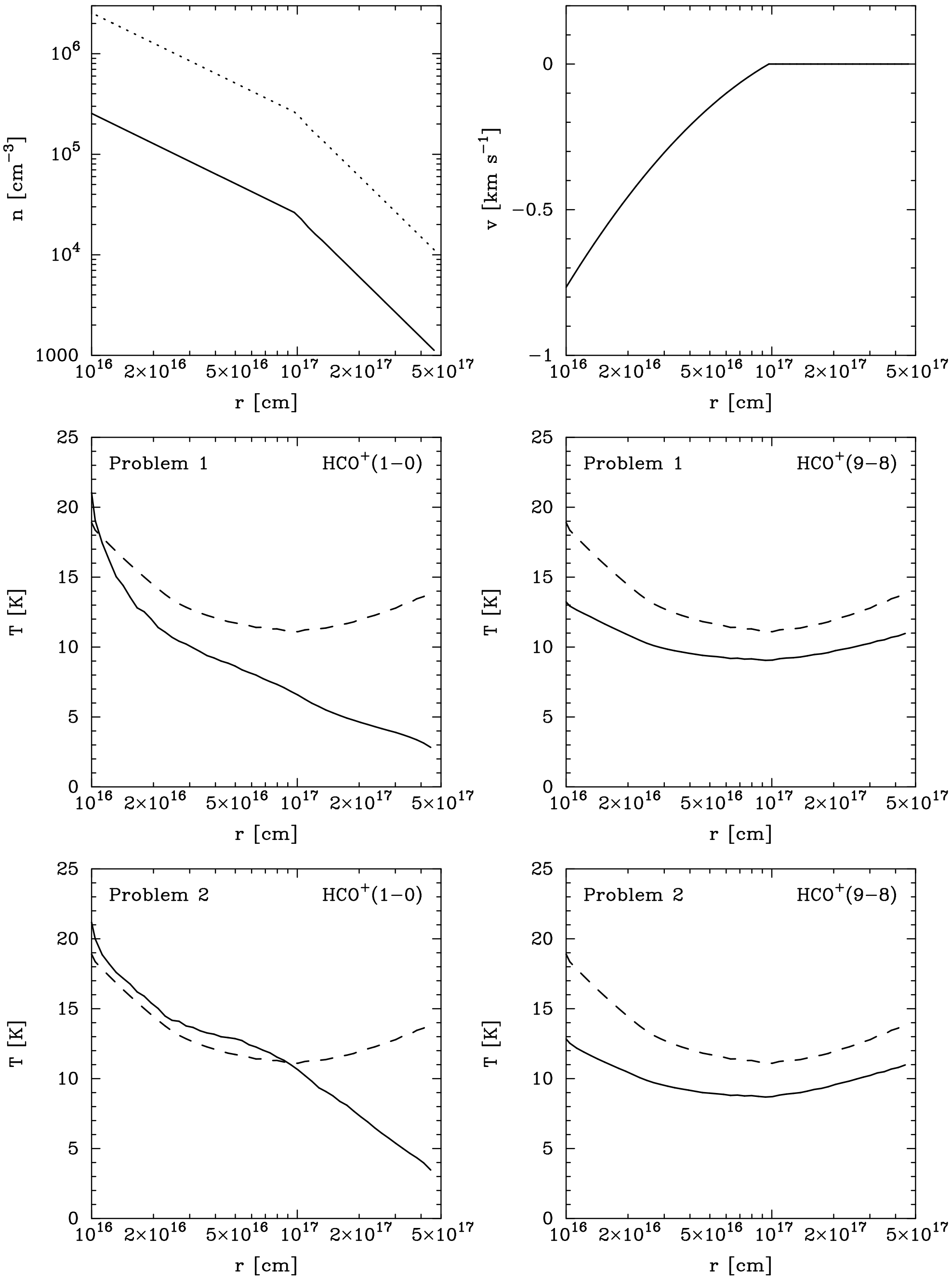

Figure 2.1: Test problems describing a collapsing cloud model. The upper left panel gives the density structure of the cloud for problem 1 (solid) and problem 2 (dotted). All other parameters describing the cloud are identical between the two problems, e.g., the velocity structure (upper right panel). Shown are also the derived excitation temperatures (solid) in two selected lines for each of the two test cases. The adopted kinetic temperature (dashed) is shown for comparison.

Chapter 3

Modelling circumstellar molecular line emission

The basic physical characteristics of a CSE, e.g., the density distribution, the gas kinetic temperature, and the gas expansion velocity, are best determined using a radiative transfer analysis of the observed CO line emission. The CO molecule is particularly well suited for this purpose, since it is difficult to photodissociate and easy to excite through collisions, and thus is a very good tracer of the molecular gas density and temperature. The standard model used to interpret the CO data is described below (see also **Paper I**). Examples of CSEs that have been modelled in CO can be found in **Papers I–V**. When the general structure of the CSE has been determined from the CO modelling, the molecular line emission from other molecular species may be investigated (**Paper VI**).

3.1 The Thesis

In **Paper I** we analyse the CO line emission from a relatively complete sample of optically bright carbon stars. Multi-transition single-dish observations and radial brightness distributions obtained from interferometer observations are used as constraints. In **Paper II** we model simultaneously CO radio and infrared line observations of a somewhat peculiar carbon star. In **Paper III** we expand the modelling to include also the ^{13}CO isotopomer, and, through comparison with photospheric results, we believe that the circumstellar ^{12}CO/^{13}CO-ratio is a good measure of the stellar ^{12}C/^{13}C-ratio. In **Paper IV** CO radio rotational lines and near-infrared rotational-vibrational lines are modelled for the well known Mira variable *o* Ceti (Mira). **Paper V** provides detailed observations and a preliminary analysis of CO line emission from a carbon star with highly episodic mass loss.

Since knowledge of the size of the emitting region is crucial for estimating abundances, and since single-dish observations do not generally resolve the sources, interferometric observations are of utmost importance. To be able to strengthen the observational constraints put on the chemistry models we have made use of the IRAM interferometer on Plateau de

Bure, France, to actually measure brightness distributions of HCN and CN line emission towards a sample of carbon stars, which spans a large mass loss rate interval (**Paper VI**). The numerical modelling of the interferometer data, using the radiative transfer code described in this thesis, and supplemented by a wealth of multi-transition single-dish data, is superior to anything that has been done before. Our radiative transfer code was modified in order to take the hyperfine splitting of these molecules and the resulting non-local line overlaps into account. Overall our results on the brightness distributions are in qualitative agreement with current theoretical models on photospheric and circumstellar chemistry when it comes to the size estimates. The results from **Paper VI** will be used in a forthcoming paper (Schöier & Olofsson 2000) to model the remaining part of the large data base presented in the **Appendix**.

3.2 The standard model

The numerical modelling of CSEs, where intricate interplays between physical and chemical processes take place, is a challenge. This applies, in particular, to the important inner regions of the CSEs, where very few observational constraints are available and our knowledge is very limited. In this analysis, we will neglect many of these complexities and assume a fairly simple, yet reasonably realistic, CSE.

In what will be referred to as "the standard model" we assume a spherically symmetric CSE that expands at a constant velocity. It is divided into a number of discrete shells, each with its own set of physical parameters describing the state of the molecular gas. The density structure, $\rho_{\mathrm{H_2}}$, (as a function of distance, r, from the central star) can then be derived from the conservation of mass

$$\rho_{\mathrm{H_2}} = n_{\mathrm{H_2}} m_{\mathrm{H_2}} = \frac{\dot{M}}{4\pi r^2 v_{\mathrm{e}}}, \tag{3.1}$$

where $\dot{M}$ is the hydrogen gas mass loss rate and v_{e} is the gas expansion velocity taken from the observed line profiles. We assume that in the CSEs of interest here the hydrogen is in molecular form in the region probed by the CO emission (Glassgold & Huggins, 1983).

The kinetic gas temperature is calculated in a self-consistent way, using the derived level populations, by solving the energy balance equation (e.g., Goldreich & Scoville 1976),

$$\frac{dT}{dr} = (2-2\gamma)\frac{T}{r} + \frac{\gamma - 1}{n_{\mathrm{H_2}} k v_{\mathrm{e}}}(H - C), \tag{3.2}$$

where γ is the adiabatic index, k the Boltzmann constant, H the total heating rate per unit volume, and C the total cooling rate per unit volume. The first term on the right hand side is the cooling due to the adiabatic expansion of the gas. Additional cooling is provided by mainly molecular line emission from CO, calculated from the derived level populations. In addition, HCN could be an important coolant in the inner parts of the envelope and will be addressed in a forthcoming paper (Schöier & Olofsson 2000).

The mechanism responsible for the observed mass loss is probably (at least for the stars of interest here) radiation pressure acting on small dust grains, which in turn are coupled to the gas (e.g., Höfner 1999). The radiation pressure on the dust grains will give them a drift velocity, $v_{\rm dr}$, relative to the gas (Gilman 1972; Goldreich & Scoville 1976; Kwan & Hill 1977)

$$v_{\rm dr} = \left(\frac{L\, v_{\rm e}\, Q}{\dot{M} c}\right)^{1/2}, \tag{3.3}$$

where L is the luminosity, Q the averaged momentum transfer efficiency, and c the speed of light (see Sahai 1990 for a more elaborate treatment). As a result of the dust-gas drift, kinetic energy of the order of $\frac{1}{2}m_{\rm H_2}v_{\rm dr}^2$ will be transfered to the gas each time a particle collides with a dust grain. This is assumed to provide the dominating heating of the gas (Goldreich & Scoville 1976; Kwan & Hill 1977). Additional heating is provided by, e.g., the photoelectric effect (Huggins et al. 1988). This heating mechanism is important in the cool, tenuous, outer parts of CSEs around high mass loss rate stars.

The size of the CO envelope is an important parameter, and the derived mass loss rate will depend on this (at least for low mass loss rate objects). The size of the circumstellar CO envelope was estimated using the modelling presented in Mamon et al. (1988). It includes photodissociation, taking into account the effects of dust-, self- and H_2-shielding, and chemical exchange reactions. In **Papers I & II** we demonstrate that the CO photodissociation calculation by Mamon et al. (1988) gives reasonably accurate results.

In our models we include both a central source of radiation and the cosmic microwave background radiation at 2.7 K. The central radiation emanates from the star itself, which may be approximated by a blackbody. In some sources, where a prominent infrared-excess is observed, fitting the spectral energy distribution with two blackbodies provide a first approximation to the radiation field that the CSE is subjected to.

This was a summary of the assumptions used in "the standard model". In what follows, we will apply this model to determine the basic parameters of the CSE around the well-known carbon star IRC+10216.

3.3 Modelling IRC+10216

As a demonstration of the usefulness of our radiative transfer code, CO line emission from the archetypical carbon star IRC+10216 (also known under its variable name CW Leo) has been modelled. The small- and large-scale structure of the molecular emission of CSEs are poorly known and much of our knowledge stems from observations of this star. IRC+10216 also provides an excellent laboratory in which to test different models.

Presented here is a self-consistent model of the observed CO line emission towards this source. The observational constraints used range from the lowest rotational transitions, as observed from the ground in the millimetre and sub-millimetre wavelength regimes, through higher rotational transitions, obtained from high altitudes using the KAO, up to the high (J∼20−30) rotational levels observable from space using ISO. These rotational lines are formed under highly different circumstances, and sample gas at very different temperatures, allowing us to trace the molecular gas throughout most of the CSE. The dynamical time scale is $\sim$10000 yr, thereby putting constraints on the mass loss history of this object.

Using the Monte Carlo method we have consistently been able to model the observed CO line emission using a constant mass loss rate of $1.5\times10^{-5}\,\mathrm{M}_\odot\,\mathrm{yr}^{-1}$, assuming a relative abundance of CO to H_2 of 1×10^{-3} and a distance of 120 pc. The expansion velocity throughout the CSE is set to $14.5\,\mathrm{km\,s}^{-1}$, as derived from the radio line profiles. When comparing our mass loss rate estimate for IRC+10216 to those obtained from other detailed radiative transfer models (Kastner 1992; Crosas & Menten 1997; Groenewegen et al. 1998; Skinner et al. 1999) we find a very good agreement, within 20 %, when adjustments for differences in f_0 and distance have been made.

We conclude that the mass loss rate experienced by IRC+10216 has not been modulated by much over the past $\sim$10000 yr. In **Paper II** the carbon star IRAS 15194-5115 was modelled in a similar way. The results for this particular object were also indicative, within the observational uncertainties, of a mass loss rate more or less constant over the past $\sim$5000 yr.

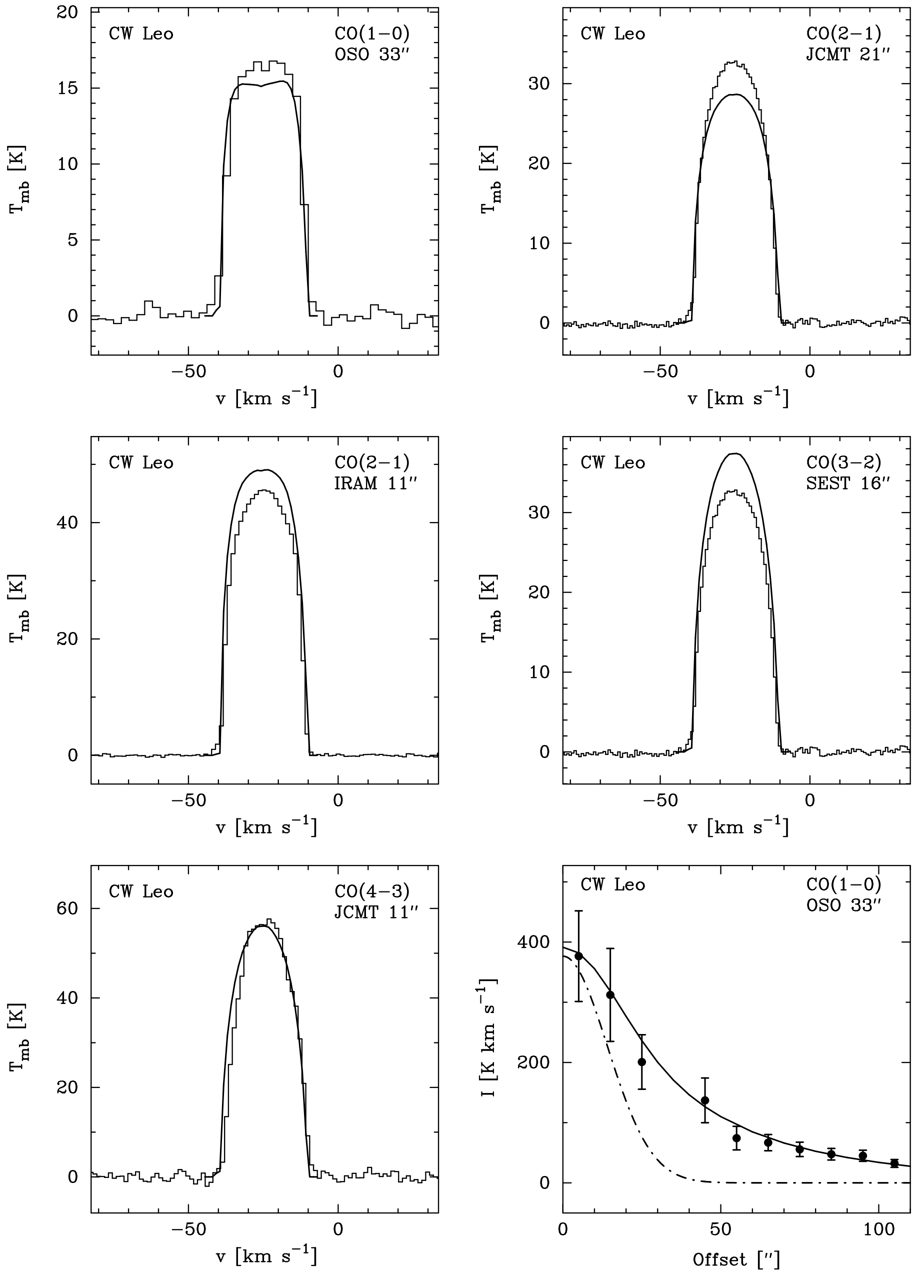

Figure 3.1: Multi-transition CO millimetre wave line emission observed towards the high mass loss rate Mira variable IRC+10216. The observed spectra (histograms) have been overlayed with the model predictions (full line) using a mass loss rate of $1.5\times10^{-5}\,\mathrm{M_\odot\,yr^{-1}}$. The transition, telescope used, and the beamsize, are given for each of the observations. Also shown are the observed radial CO(J=1→2 brightness distribution overlayed by the result from the model (full line). The circular beam used in the radiative transfer analysis is indicated by the dot-dashed line.

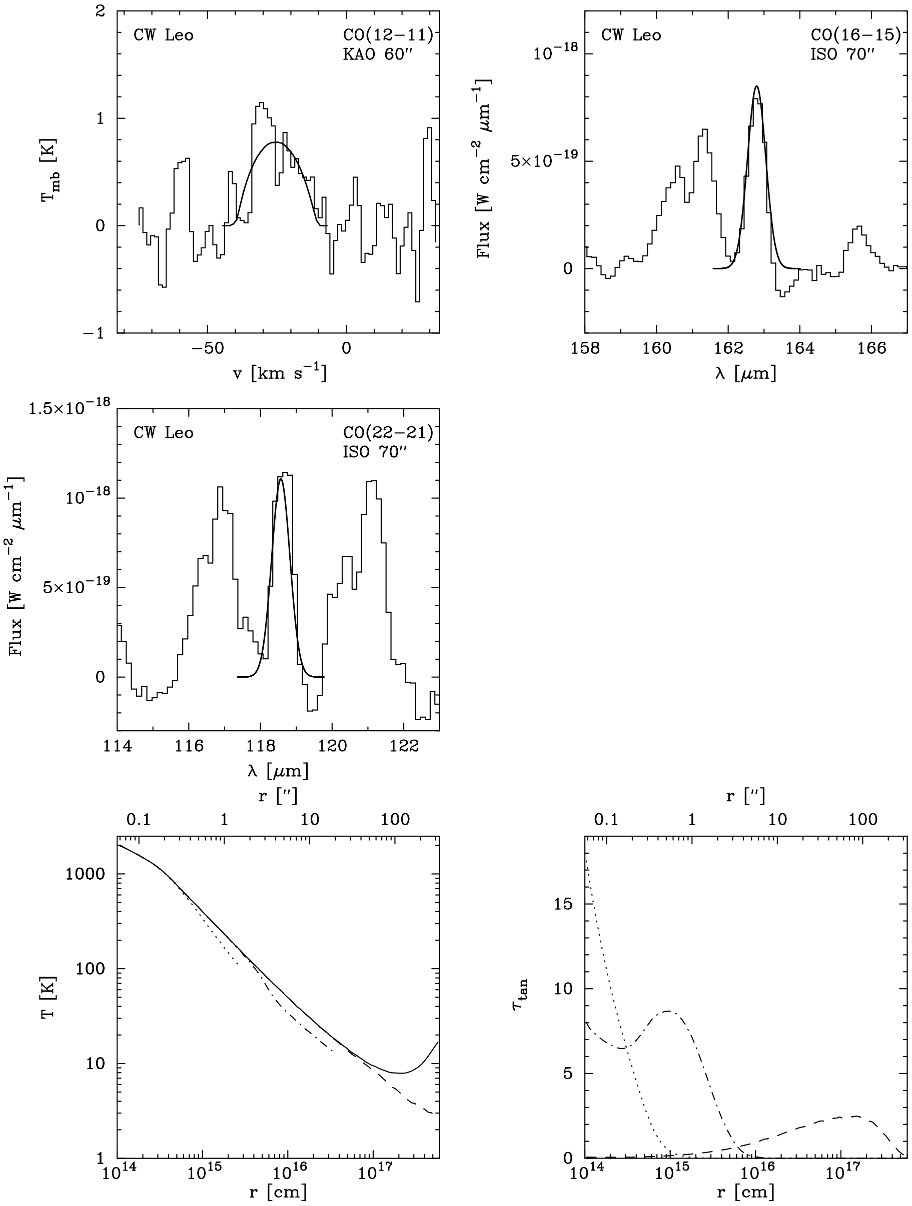

Figure 3.2: Multi-transition CO line emission observed towards the high mass loss rate Mira variable IRC+10216. The observed spectra (histograms) have been overlayed with the model predictions (full line) using a mass loss rate of $1.5{\times}10^{-5}\,\mathrm{M}_{\odot}\,\mathrm{yr}^{-1}$. The transition, telescope used, and the beamsize, are given for each of the observations. In the temperature panel the excitation temperatures of the J=1→0 (dash), the J=12→11 (dash-dot), and the J=31→30 (dot) transitions are shown. The solid line shows the gas kinetic temperature derived from the excitation analysis. Also shown are the tangential optical depths in these three transitions.

Chapter 4

Svensk sammanfattning

Den föreliggande avhandlingen behandlar en detaljerad studie av röda jättestjärnor. Döende stjärnor av röd jättetyp förlorar mängder av materia genom en intensiv stjärnvind. Denna materia är berikad på tunga grundämnen och dessa stjärnor bidrar på detta sätt till galaxernas kemiska utveckling. Man beräknar att alla stjärnor i massintervallet 1-10 solmassor går igenom detta stadium, dvs en avsevärd del av alla stjärnor i en galax. Vår egen sol beräknas passera detta stadie om ungefär åtta miljarder år. Således kan studiet av röda jättar ge oss ledtrådar till det slutliga ödet för vårt eget solsystem.

Den primära observationella konsekvensen av materieförlusten är bildandet av ett, för ljuset skymmande, cirkumstellärt hölje kring stjärnan. I de extrema slutstadierna är studiet av detta hölje det enda sättet att följa den fortsatta utvecklingen hos stjärnan. Molekyler i höljet sänder mestadels ut strålning med lång våglängd, radiovågor, vilka kan detekteras med radioteleskop. I avhandlingen presenteras en stor mängd observationalla data av denna art.

Genom användandet av en detaljerad modell för strålningstransport i dessa cirkumstellära höljen kan noggranna uppskattningar av mängden materia som stjärnan förlorar göras. Det är också möjligt att bestämma med vilken hastighet materien kastas ut från stjärnans atmosfär samt förekomsten av olika molekyler. Dessa resultat sätter viktiga tvång på modeller för stjärnutveckling.

Enligt våra beräkningar för en viss typ av röda jättar, de så kallade kolstjärnorna, så är förmodligen dessa stjärnor viktiga bidragsgivare av material till den kemiska utvecklingen i vår galax. Ironiskt nog så verkar kolstjärnorna dock inte vara särskilt viktiga just för ämnet kol i sig.

Genom att kombinera observationer gjorda i olika våglängdsområden kan den kringliggande gasen studeras på olika avstånd från centralstjärnan. Olika lager av stjärnhöljet, skapade vid olika tidpunkter, är då möjliga att specialstudera. Detta medför en form av stjärnarkeologi, där stjärnans massförlusthistorik kan registreras. I avhandlingen undersöks bland annat två röda jättar med hjälp av denna metodik.

Acknowledgements

I would like to first of all thank my supervisor **Prof. Hans Olofsson** for his support and concern, always taking the time to discuss some particular problem. His broad scientific knowledge and intuition have indeed been a continuous source of inspiration.

Dr. Nils Ryde and **Dr. Michael Lindqvist** are thanked for creating a creative and pleasant atmosphere, and for fruitful collaboration.

Dr. Per Bergman is tanked for kindly providing me with a modified version of the original Monte Carlo code by Bernes, adapted to expanding envelopes, and for generous help during some of the observations at Onsala.

I am pleased to thank **Dr. Lars-Åke Nyman** and **Dr. Lars E.B. Johansson** for invaluable assistance during my observing runs at SEST and OSO, respectively.

Prof. Bengt Gustafsson and **Dr. Kjell Eriksson** are thanked for stimulating and enlightening discussions.

Drs. Franz Kerschbaum, **Claudine Kahane**, and **Robert Lucas** are gratefully acknowledged for valuable scientific input.

I am grateful to all the people at the Stockholm Observatory for creating a friendly atmosphere and making these years a pleasant and interesting time. My fellow graduate students **Andreas Andersson**, **Tomas Dahlén**, and **Felix Ryde** are acknowledged for all the good times both at and outside the Observatory.

Thanks to friends and family, in particular my wife **Anna** for her support and my daughter **Felicia** for making life so much fun.

Financial support from the **Swedish Natural Science Research Council (NFR)** is gratefully acknowledged.

Stockholm in May 2000

Fredrik L. Schöier

Bibliography

Bergman P., 1985, Diploma thesis, Onsala Space Observatory

Bergman P., Carlström U., Olofsson H., 1993, A&A 268, 685

Bernes C., 1979, A&A 73, 67

Blöcker T., 1995, A&A 297, 727

Boothroyd A. I., Sackmann I. J., Ahern S. C., 1993, ApJ 416, 762

Busso M., Gallino R., Wasserburg G. J., 1999, ARA&A 37, 239

Cannon C. J., 1985, *The transfer of spectral line radiation*, Cambridge University Press

Crosas M., Menten K. M., 1997, ApJ 483, 913

Deutsch, A. J., 1956, ApJ, 123, 210

Forestini M., Charbonnel C., 1997, A&AS 123, 241

Gilman R. C., 1972, ApJ 178, 423

Glassgold A. E., Huggins P. J., 1983, MNRAS 203, 517

Goldreich P., Scoville N., 1976, ApJ 205, 144

González-Alfonso E., Cernicharo J., 1993, A&A 279, 506

Greaves J. S., Holland W. S., 1997, A&A 327, 342

Groenewegen M. A. T., van Der Veen W. E. C. J., Matthews H. E., 1998a, A&A 338, 491

Gustafsson B., Eriksson K., Kiselman D., Olander N., Olofsson H., 1997, A&A 318, 535

Habing H. J., 1996, ARA&A 7, 97

Höfner S., 1999, in *Asymptotic Giant Branch Stars*, T. Le Bertre, A. Lèbre, C. Waelkens (eds.), IAU Symp. No. 191, Astronomical Society of the Pacific, p. 159

Huggins P. J., Olofsson H., Johansson L. E. B., 1988, ApJ 332, 1009

Iben I. Jr., Renzini A., 1983, ARA&A 21, 271

Kastner J. H., 1992, ApJ 401, 337

Kwan J., Hill F., 1977, ApJ 215, 781

Kwok S., 1993, ARA&A 31, 63

Lambert D. L., Gustafsson B., Eriksson K., Hinkle K. H., 1986, ApJS 62, 373

Lattanzio J. C., Forestini M., 1999, in *Asymptotic Giant Branch Stars*, T. Le Bertre, A. Lèbre, C. Waelkens (eds.), IAU Symp. No. 191, Astronomical Society of the Pacific, p. 31

Mamon G. A., Glassgold A. E., Huggins P. J., 1988, ApJ 328, 797

Neri R., Kahane C., Lucas R., Bujarrabal V., Loup C., 1998, A&AS 130, 1

Olofsson H., Eriksson K., Gustafsson B., Carlström U., 1993, ApJS 87, 267

Olofsson H., 1996a, Ap&SS 245, 169

Olofsson H., Bergman P., Eriksson K., Gustafsson B., 1996b, A&A 311, 587

Olofsson H., 1997, in *Molecular Astrophysics: Probes & Processes*, E. van Dishoeck (ed.), IAU Symp. No. 178, Kluwer, Dordrecht, p. 457

Olofsson H., Bergman P., Lucas R., et al., 2000, A&A 353, 583

Prantzos N., Aubert O., Audouze J., 1996, A&A 309, 760

Sackmann I. -J., Boothroyd A. I., Kraemer K. E., 1993, ApJ 418, 457

Sahai R., 1990, ApJ 362, 652

Schöier F. L., Olofsson H., 2000, in prep.

Schönberner D., 1983, ApJ 272, 708

Sedlmayr E., 1990, in *From Miras to Planetary Nebulae: Which path for Stellar Evolution?*, M. O. Mennessier and A. Omont (eds.), Editions Frontiérs, p. 179

Shu, F. H., 1977, ApJ 214, 488

Skinner C. J., Justtanont K., Tielens A. G. G. M., et al., 1999, MNRAS 302, 293

Solomon P., Jefferts K. B., Penzias A. A., Wilson R. W., 1971, ApJL 163, L53

Wallerstein G., Knapp G. R., 1998, ARA&A 36, 369